Available online at www.sciencedirect.com
SCIENCE DIRECT®

Journal of the European Ceramic Society 23 (2003) 19–27

www.elsevier.com/locate/jeurceramsoc

High temperature sintering of SiC with oxide additives: III. Quantitative vaporization of SiC–Al_2O_3 powder beds as revealed by mass spectrometry

S. Baud[a], F. Thévenot[a,b], C. Chatillon[b,*]

[a]*Ecole Nationale Supérieure des Mines de Saint-Etienne, 158 cours Fauriel, 42023 Saint-Etienne Cedex 2, France*
[b]*Laboratoire de Thermodynamique et de Physico-Chimie Métallurgiques (CNRS UMR5614-INPG-UJF), ENSEEG, BP. 75, 38402 Saint Martin d'Hères, France*

Received 20 August 2001; received in revised form 25 February 2002; accepted 11 March 2002

Abstract

This high temperature mass spectrometric study is aimed at the quantitative vaporization of powder beds of SiC–Al_2O_3 and related triphasic SiC–Al_2O_3–C and SiC–Al_2O_3-Si powder mixtures. The quantitative evaluation of reaction enthalpies showed that the different vaporization processes are not equilibrium processes and all the vaporization reactions are kinetically hindered. The multiple Knudsen cell method is used to determine directly the condensation coefficients of the Al(g), Al_2O(g), CO(g) and SiO(g) species. Further, the comparison with previous equilibrium pressures calculated using thermodynamics allows the calculation of the evaporation coefficients of these species from the condensation coefficients and the measured mass spectrometric pressures. Supersaturated or undersaturated resultant pressures for each species are used as a criteria in the choice of suitable powder beds.

Keywords: Evaporation coefficients; Knudsen cell; Mass spectrometry; SiC(Al_2O_3); Vaporisation

1. Introduction

The thermodynamic analysis of the vaporization behavior[1] of the SiC–Al_2O_3 pseudo-binary system showed that the main vaporization reaction is,

$$Al_2O_3(s) + 2SiC(s) + Al_2O(g) \Longleftrightarrow 4Al(g) + 2CO(g) + 2SiO(g) \quad (1)$$

meanwhile other species like AlO(g) or Si(g) and Si_2C(g) are minor species (less than 10^{-3}) of total pressure. The gas composition—referred to the basic Al–C–O–Si quaternary system—of any Al_2O_3 + SiC mixture is located in the pseudo-binary Al_2O_3–SiC section. Any matter loss by the gas phase cannot lead to a condensed residue with a final composition out of the pseudobinary section. The vaporization behaviour can be termed as pseudo-azeotropic or pseudo-congruent because gas composition ratios as Si/C = 1/1 or Al/O = 2/3 are constant during the vaporization[1] (all the gaseous species being taken into account). Consequently any matter loss will move the condensed phase composition along the pseudo-binary SiC–Al_2O_3 section. For mixtures with small alumina content,[1] the evolution is toward pure SiC, and this feature explains the alumina losses observed during sintering.

The gas phase analysis, performed qualitatively in the preceding paper[2] by Knudsen-cell mass spectrometry, confirmed that the main gaseous species are those predicted by thermodynamics, and that the impurities—including small excess SiO_2 or small excess C—are distilled during the heating stage at intermediate temperatures. The comparison between different powder beds, loaded in different cells and for different SiC/Al_2O_3 compositions, using the multiple cell method showed that, contrary to thermodynamics, the partial vapor pressures were not constant for the SiC–Al_2O_3, the SiC–Al_2O_3-C or SiC–Al_2O_3–Si systems when composition is varied. This feature suggests that the vaporization is kinetically hindered, and some condensation and

* Corresponding author.
E-mail address: chatillo@ltpcm.inpg.fr (C. Chatillon).

0955-2219/02/$ - see front matter
PII: S0955-2219(02)00069-9

evaporation coefficients are lower than unity. Unity corresponds to thermodynamic control of the net evaporation process in the cells. The effect of these coefficients is generally to decrease the partial pressures measured with effusion cells. This paper is aimed to the determination of these coefficients as well as evaluation of their impact on powder bed vaporization behavior.

2. Analysis by conventional quantitative vaporization

2.1. Vaporization reactions and samples

Conventional Knudsen cell mass spectrometric experiments[3–6] were run using single cells as described in Fig. 1 of the preceding paper.[2] The samples, the container and the effusion orifice characteristics are presented in Table 1. For samples of the $SiC–Al_2O_3$ pseudobinary section, the main vaporization reaction is reaction (1). For the samples corresponding to triphasic domains—excess of C or Si—the total vaporization reactions can be written as,

$$SiC(s) + Al_2O_3(s) + CO(g) + 4Al(g) \Longleftrightarrow SiO(g) + 2C(s) + 3Al_2O(g) \quad (2)$$

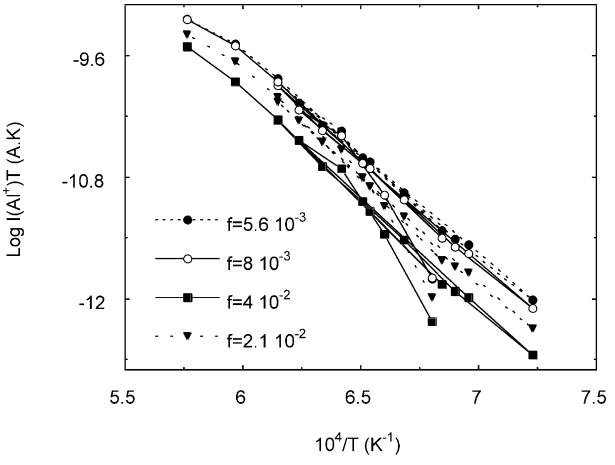

Fig. 1. Evolution of the decimal logarithm of vapor pressure of Al(g)—proportional to the IT product—as a function of the inverse of temperature as measured for four cells with different f factors (see text) in a multiple cell experiment run with mixtures SiC + Al_2O_3.

and

$$SiC(s) + 2Al_2O_3(s) + Si(s) + 2Al(g) \Longleftrightarrow 2SiO(g) + CO(g) + 3Al_2O(g) \quad (3)$$

The molar fractions in the samples were chosen in agreement with these two reactions in order to favor equilibrium conditions when kinetic limitations exist at grains contacts as previously observed for $Si–SiO_2$ mixtures.[3]

2.2. Knudsen cell mass spectrometric method

The molecular beam, effused from the orifice of the Knudsen cell and sampled along the normal to the orifice by small apertures, crosses the ionization chamber of the mass spectrometer. An electron beam ionizes the molecules of the beam, and the ions are accelerated by an electric field (4600 V), deflected by a magnetic field (radius 30.2 cm, 90°) and finally collected on a secondary electron multiplier. The detection of the ionic intensity $I^+{}_i$ is performed by a pulse counting device. The basic mass spectrometric relation,

$$p_i = I_i^+ T / S_i \quad (4)$$

relates the measured ionic intensity I_i^+ to the partial pressure p_i of the parent molecule in the Knudsen cell,[3–7] the temperature T of the cell and the mass spectrometric sensitivity S_i. In addition, the effusion mass loss during the experiment is written according to the Hertz–Knudsen equation,[3–7]

$$\frac{dNi}{dt} = \frac{p_i s C}{\sqrt{2\pi M_i R T}} \quad (5)$$

in which dN_i/dt is the number of moles i effusing by unit time, s and C the cross sectional area and Clausing coefficient of the orifice, M_i the molar mass of the effusing species i, and R the gas constant. Combining relations (4) and (5) allows the direct relation between the total mass loss during an experiment Δm_i and the parameters of the mass spectrometric experiment, I_i^+, T and S_i:

Table 1
Experiments run quantitatively using single conventional Knudsen effusion cells

Experiment label	Powder nature	Crucible material	Effusion orifice[a](mm)
$SiCAl_2O_3$-01S	SiC (norton) + 50% (mol) Al_2O_3	Al_2O_3	$h=2.02$ $d=2$
$SiCAl_2O_3$-02S	25% (mol) SiC (norton) + 25% Al_2O_3 + 50%C	Graphite (SiC coated)	$h=2$ $d=1.72$
SiC Al_2O_3-03S	25% (mol) SiC (norton) + 50% Al_2O_3 + 25%Si	Graphite (SiC coated)	$h=2$ $d=1.72$
SiC Al_2O_3-04S	SiC (carborundum) + 50% (mol) Al_2O_3	Graphite (SiC coated)	$h=2$ $d=2$

[a] h is the length of the cylindrical orifice walls, d the diameter.

$$\Delta m_i = \frac{sC}{\sqrt{2\pi R}} x \frac{\sqrt{M_i}}{S_i} \sum_j I_i^+ \sqrt{T} \mathrm{d}t \quad (6)$$

j being the different temperature plateaus for measurements (integration between the plateaus is done applying the trapezoidal method to the $I_i^+\sqrt{T}$ function). This method of calibration was used systematically in order to determine S_i after weighing the crucible before and after the experiments. Supplementary calibrations with a silver foil ($\cong 5$ mg) evaporated at the beginning of the run were used. The sensitivity of the mass spectrometer for Ag was thus calculated by observation of the silver melting temperature using the mass spectrometric relation (4) and the known thermodynamic values for saturated pressure of silver.[8]

In our experiments the total measured mass loss corresponds to four effused species that have similar partial pressures and we needed to evaluate relative sensitivity values by an independent way and relation (6) becomes:

$$\Delta m = \frac{sC}{\sqrt{2\pi R}} \cdot \frac{\sqrt{M_1}}{S_1} \times \left[\sum_j I_i^+ \sqrt{T} \mathrm{d}t + \sum_{i=2}^{n} \left(\frac{S_1}{S_i} \sqrt{\frac{M_i}{M_1}} \sum_j I_i^+ \sqrt{T} \mathrm{d}t \right) \right] \quad (7)$$

the species 1 being chosen as the reference (silver is used also as a secondary one). The sensitivity ratios in our case are:

$$\frac{S_1}{S_i} = \frac{\sigma_1 A_1}{\sigma_i A_i} \quad (8)$$

σ_i being the ionization cross section either issued from earlier experiments or from literature (Table 2), A_i being the isotopic abundance calculated exactly from the atoms one's.

Other parameters cancel. The sensitivities determined by mass loss or by reference to silver differed by less than 2.2%, meanwhile the evaluation by simple derivation on the basis of relation (7) of the total absolute uncertainty on each sensitivity was $\pm 18\%$.

Table 2
Ionization cross-sections or their ratios for 30 V ionizing electrons

Gaseous molecule	Cross-section σ_i (Å^2)	(References)
Al	9.7	(9)
Al_2O	12.513	$\frac{\sigma_{Al_2O}}{\sigma_{Al}} = \frac{\sigma_{Ga_2O}}{\sigma_{Ga}} = 1.29 \pm 0.13$ (10)
CO	1.05	(11)
Ag	5.16	(9)
SiO	7.242	$\frac{\sigma_{SiO}}{\sigma_{Ag}} = 1.42$ (3)

2.3. 2nd and 3rd law calculations

The basic mass spectrometric relation (4) gives access to partial pressures for each effused species and consequently to equilibrium constants. The use of the second and third laws of thermodynamics[4–6,12,13] lead to the enthalpies of the observed reactions.

The second law method leads to the Clausius–Clapeyron equation,

$$\mathrm{d}\ln Kp/\mathrm{d}(1/T) = -\Delta_r H^\circ(T,\ \text{mean})/R \quad (9)$$

or using the basic mass spectrometric relation,

$$-\Delta_r H^\circ(\text{mean } T) = -R\mathrm{d}\ln \prod_i \left(I_i^+ T\right)/\mathrm{d}(1/T) + R\mathrm{d}\ln\left(\prod_i S_i\right)/\mathrm{d}(1/T) \quad (10)$$

As the experiments are run in such a way that the sensitivity is maintained constant, the last term can be discarded, and calibration of the apparatus is not necessary when using the 2nd law method.

The third law calculations need the a priori knowledge of the standard entropies of all the species in the measured reactions via the relation,

$$\Delta_r G^\circ(T) = -RT\ln Kp = \Delta_r H^\circ(T) - T\Delta_r S^\circ(T) \quad (11)$$

which is more often used with a fixed reference temperature (0 or 298 K) as:

$$\Delta_r H^\circ(298K) = -RT\ln Kp(T) - T\Delta fef^\circ(T) \quad (12)$$

The free energy function—defined as $\text{fef} = -\left(G_T^0 - H_{28K}^0\right)/T$—is a combination of entropy and enthalpy increments obtained from thermodynamic tables[12–14] and stored for our purpose in the SGTE data bank.[15] The calculation of reaction enthalpies by the third law method requires the determination of the equilibrium constant Kp and consequently of partial pressures through the calibration of the mass spectrometer.

2.4. Results

Calculations using the second and third law methods—the second law one being recalculated at 298 K by use of enthalpic increments—are presented in Table 3 and compared with the values taken from thermodynamic tables for the same vaporization reactions. As these reactions are based on well-known compounds and gaseous species, results should be comparable within their uncertainty limits. This is not the case except perhaps for some third law results that may approach the calculated values with thermodynamic

reference tables. The second law results are far from the expected values.

The inconsistent results between the two methods as well as the large discrepancies observed with tabulated equilibrium values show that some kinetic barrier occurs in the vaporization process. We observed already such behavior with Si–SiO_2 powders,[3] the discrepancies were accounted for by the effect of the evaporation coefficient on the vapor pressures. The multiple cell observations in the preceding paper[2] reinforce this assumption. Here we further use this latter method in the determination the evaporation and condensation coefficients which reflect the kinetic barriers.

3. Evaporation and condensation coefficients of powder beds

3.1. Definition of the coefficients

For free or Langmuir vaporization of a surface under perfect vacuum—no molecules come back to impinge the surface—the vaporization flow is related to the maximum Knudsen flow vaporizing at equilibrium:

$$\phi_i(L) = \alpha_i \frac{p_i S}{\sqrt{2\pi M_i RT}}. \tag{13}$$

The evaporation coefficient α_i,—specific to each i species—is equal to 1 at equilibrium, and lower than 1 when a vaporization step is kinetically hindered.

Conversely, for a flow of molecules that impinges on a surface, a condensation coefficient β_i can be defined that relates the maximum flow condensing at equilibrium—equal to the equilibrium vaporization flow at the substrate temperature—to the impinging flow. These coefficients are called gross evaporation and condensation coefficients.[16,17] The impact of these coefficients on Knudsen measurements was first analyzed by Motzfeld[18] and Whitman[19] with the assumption $\alpha = \beta$.

The Motzfeld relation relates the measured pressure p_m—obtained from the measured Knudsen flow by the mass spectrometer—to the hypothetical equilibrium pressure p_{eq} at the vaporizing surface, through the cell geometry (orthocylindrical cells) and the evaporation coefficient,

$$p_{eq} = p_m\left(1 + \frac{f}{\alpha}\right) \tag{14}$$

Here f is the ratio of effective effusing area sC to cell cross sectional area. This relation applies for each gaseous species independently since there are no collisions in the cell other than on the walls. For processes that are far from equilibrium, and taking into account a gross evaporation coefficient that differs from the gross condensation value, Chatillon et al.[20] recalculated this relation to be,

$$p_{eq}\frac{\alpha}{\beta} = p_m\left(1 + \frac{f}{\beta}\right) \tag{15}$$

For such a situation, we cannot extrapolate to the null orifice ($f \to 0$) size as discussed by Rosenblatt[21] since the kinetic mechanisms may change when considering the equilibrium situation for a closed orifice. Thus, we use the multiple cell method[3,22] to determine these coefficients within a rather small f range with the assumption that the kinetic limiting step is the same for all the cells with slightly different f factors.

3.2. Determination with the multiple cell method

The multiple cell method is used to compare the effused flows—or measured pressures—coming from cells with different orifice sizes. The existence of

Table 3
2nd and 3rd law calculations of the reaction enthalpies at 298 K as determined by conventional mass spectrometric single cell experiments and comparison with tabulated data

Studied system (powder bed)	Reaction (Nr)	ΔH_r^0(298.15) janaf[8] (kJ mol^{-1})	ΔH_r^0(298.15) Gurvich[9] (kJ mol^{-1})	ΔH_r^0(298.15) (kJ.mol^{-1}) 2nd law	ΔH_r^0(298.15) (kJ.mol^{-1}) 3rd law
SiC (norton) + 50% (mol) Al_2O_3	(1)	2860.89±31.84	2867.047±27.31	2685.51±85.21[a]	2931.02±22.27[b]
SiC (carborundum) + 50% (mol) Al_2O_3	(1)	2860.89±31.84	2867.047±27.31	2772.33±61.89	2911.48±13.21
25% (mol) SiC (norton) + 25% Al_2O_3 + 50%C	(2)	2.96±54.73	−7.691±67.31	−111.92±54.74	−1115.33±80.33
	(1)	2860.89±31.84	2867.047±27.31	2589.04±95.4	2892.99±35.53
25% (mol) SiC (norton) + 50% (mol) Al_2O_3 + 25% Si	(3)	2016.58±54.77	2006.95±66.75	1471.65±121.6	782.99±54.5
	(1)	2860.89±31.84	2867.047±27.31	2040.82±155.61	2777.91±61.13

[a] Standard deviation on the slope (2nd law).
[b] Standard deviation of the mean value (3rd law).

evaporation or condensation coefficients is straigthforward when measuring the same sample and observing the pressure decrease for larger orifices according to relations (14) or (15) when f increases.[3,20,22]

In a first step we compare different cells (i) to one cell taken as a reference (ref)—usually the smallest orifice—and combining relation (15) with the basic mass spectrometric relation (4),

$$\beta_i = (\text{or } \alpha_i \text{ if } \beta_i = \alpha_i) = \frac{f_i - f_{\text{ref}} \dfrac{I_i}{I_{\text{ref}}}}{\dfrac{I_i}{I_{\text{ref}}} - 1} \tag{16}$$

β_i are determined for each species and for each temperature plateau.

In a second step and according to relation (15), the evaporation coefficient α_i can be known only if independent thermodynamic values allow the calculation of the equilibrium pressure p_{eq}, meanwhile a calibration procedure is needed to deduce the measured pressure p_m from ionic intensities as already explained.[20,22] At that time, using the preceding β_i value, the known p_{eq} and the measured p_{m} pressures, we can compare according to relation (15) the $p_{\text{m}}\left(1+\frac{f}{\beta}\right)$ recalculated products with p_{eq}: if these quantities are equal, $\alpha=\beta$. If not, we calculate α from their ratio according to relation (15).

For the specific case of the pseudobinary $SiC–Al_2O_3$ vaporization, we first should define the reference equilibrium situation, that is the real equilibrium vaporization of this system. Indeed, this was a part of the basic motivation for our first paper which dealt with the vaporization behavior calculated by thermodynamics.[1] Thus the calculated congruent equilibrium vaporization in Knudsen conditions is the reference behavior for determining the evaporation and condensation coefficients in this work. For the triphasic powders, $SiC–Al_2O_3$–(C or Si), we used the triphasic equilibrium pressures.

3.3. Determination of the condensation and evaporation coefficients

The multiple cell used (see Fig. 2 in Ref. 2) is loaded with four dense graphite cells (crucibles + lids), the geometrical characteristics of which are presented in Table 4. The measured products I_i^+T (proportional to p_i) are presented in Fig. 1 in the usual manner for partial pressures—as a function of the inverse of temperature. We observe some deviation from a linear relationship at the beginning of the experiment, already discussed in the preceding paper, and a systematic pressure decrease in the high temperature range (when compared to the expected linear relationship in thermochemistry) which is accompanied by smaller differences between cells. The phenomenon may be attributed to at least three processes:

- an increasing collision number in the gas phase of the Knudsen cell[22] allowing homogeneous gas phase kinetics to occur. Part of the observed flow is thus coming increasingly from direct gaseous collisions that may be closer to equilibrium values.
- a modification of the flow regime[17] in the cell leading usually to apparent lower values for evaporation coefficients due to molecules coming back to the surface without any collision on the walls.
- an increasing saturation of adsorbed species at the surface[17] of the sample that can modify the surface adsorption kinetics, usually leading to increasing values for the coefficients.

To avoid any coupling between surface kinetics and mass flow in the mass spectrometric observations, we systematically discarded data at temperatures higher than 1667 K ($10^4/T<6$) in the evaluation of these coefficients. But yet, the coefficients values at the surface remain available for further calculations of transferts at the interface solid-gas. An example of β determination is presented in Fig. 2, obtained by a comparision between two cells. The results from other cell comparisons were not significantly different. We retain in this work the coefficients that correspond to cells similar to those single cells we shall use for the α determinations in experiments with calibration procedures (see further).

The mass spectrometric experiments were performed in the 1350–1750 K range—ranging from the mass spectrometric detection threshold to the free gas collisions in the cell orifice limit. As we need extrapolated values for our β coefficients at the temperature of the sintering process, we present mean values and least square fitted values according to the Arrhenius law[23] in Table 5. Four different runs were performed, each corresponding to different powder beds, including triphasic

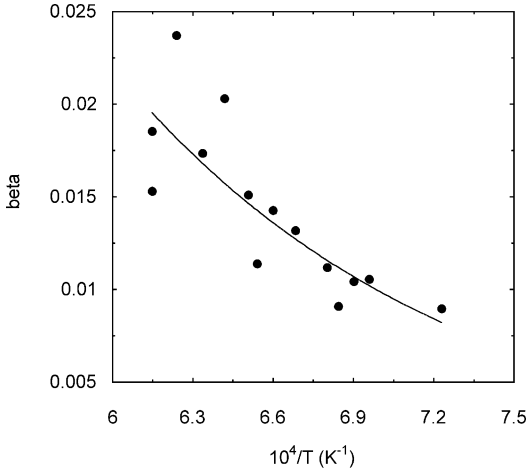

Fig. 2. Evolution of the condensation coefficient β as a function of the inverse of temperature as determined in a multiple cell experiment by comparison between two cells loaded with the same $SiC–Al_2O_3$ sample and fitted with two different effusion orifices.

beds, but with the same sample in each four cells of the multiple cell block.

We observe (Table 5) that the condensation coefficients are generally in the same range (1 to 4)10^{-2} except for (i) the CO(g) on the triphasic mixture with silicon, β_{CO} at 1500 K 10 times the value of β_{CO} of the other mixtures, (ii) the Al_2O(g) still on the triphasic mixture with silicon, the β at 1500 K $\sim 3\times10^{-3}$ value increasing to 2×10^{-2}. It seems thus that the silicon "catalyzes" the CO and Al_2O incorporation to surface reactions.

Table 4
Geometrical parameters of our effusion cells used in the multiple cell device and their associated *f* ratio (see text)

Crucible diameter (mm)	Effusion orifice diameter (mm)	Wall length of the orifice (mm)	f = ratio sC/S (see text)
16	3	2	2.1×10^{-2}
13	3	1	4×10^{-2}
16	2	4	5.6×10^{-3}
16	2	2	8×10^{-3}

Using the β least square fits (Table 5), the measured pressures p_m (part 2.4 which led to Table 3 results with second and third law calculations) are corrected using relation (15) with the correct *f* factor, and the right side of (15) is compared in Fig. 3 with calculated congruent equilibrium pressures for SiC–Al_2O_3 samples, including the two triphasics, as done in Ref. 1. We observe systematic differences showing that the evaporation and condensation coefficients have different values for all the gaseous species.

Knowing the equilibrium partial pressures and the β coefficients (fitted values), we then calculated the evaporation coefficients α. These are presented in Table 6 in the same manner as for the condensation coefficients.

Conversely to the β coefficients, the α coefficients vary largely by factors of 10–1000. Ratio of the evaporation and the condensation coefficients (Table 7) reveals some different saturation state (super or under saturation) of the surface. For $\alpha/\beta<1$ the surface is supersaturated for this species while the gas phase is not. The converse holds for $\alpha/\beta>1$. Thus, according to Table 7, for the

Table 5
Condensation coefficients β as determined from our multiple cell experiment and for each gaseous species Al(g), Al_2O(g), SiO(g) and CO(g) and for different powder beds

Studied system (powder bed)	Method for β calculation	β (Al)	β (Al_2O)	β (SiO)	β (CO)
SiC (Nor.) + Al_2O_3	β (mean[a])	0.0117±0.0055	0.0081±0.0111	0.0118±0.0101	0.0382±0.0437
	ln β (fit)	0.989–8009/T	5.663–17 027/T	−4.733 + 274/T	−6.032 + 3844/T
	β (at 1500 K)	0.0129	0.0034	0.0106	0.0311
SiC (Car.) + Al_2O_3	β (mean)	0.0151±0.0102	0.0069±0.0071	0.0497±0.0409	0.0225±0.0164
	ln β (fit)	1.633–9341/T	3.375–13656/T	1.631–7095/T	−16.118 + 18 635/T
	β (at 1500 K)	0.0101	0.0033	0.0451	0.0249
SiC (Nor.) + Al_2O_3 + C	β (mean)	0.0222±0.0244	0.0179±0.0342	0.331±0.0423	0.0385±0.0538
	ln β (fit)	1.915–9416/T	7.412–19 403/T	−13.122 + 13961/T	−7.824 + 5949/T
	β (at 1500 K)	0.0127	0.004	0.022	0.0211
SiC (Nor.) + Al_2O_3 + Si	β (mean)	0.0674±0.0665	0.0495±0.0534	0.0316±0.0529	0.084±0.0644
	ln β (fit)	−7.601 + 6042/T	−10.414 + 9888/T	−21.64 + 26 039/T	−8.112 + 8900/T
	β (at 1500 K)	0.0281	0.0219	0.0138	0.113

[a] Mean is a mean value and its standard deviation calculated whatever is the temperature of the measurements.

Table 6
Evaporation coefficients α for each gaseous species as determined from our partial vapour pressures obtained by single cell experiments (Table 1) and from a method of calculation (see text) that takes into account the preceding condensation coefficients as determined in Table 5

Studied system (powder bed)		α (Al)	α (Al_2O)	α (SiO)	α (CO)
SiC (Nor.) + Al_2O_3	α (mean[a])	0.0134±0.0026	0.0078±0.0023	0.0075±0.0051	0.0130±0.0032
	ln α (fit)	−5.185 + 1286/T	−8.112 + 5002/T	−8.112 + 4442/T	−3.14–1892/T
	α (at 1500 K)	0.0132	0.0084	0.0058	0.0123
SiC (Car.) + Al_2O_3	α (mean)	0.0135±0.0019	0.0113±0.0019	0.0050±0.0010	0.0993±0.1124
	ln α (fit)	−2.616–2572/T	−5.745 + 1889/T	−2.381–4442/T	−13.122 + 16 061/T
	α (at 1500 K)	0.0132	0.0113	0.0048	0.0894
SiC (Nor.) + Al_2O_3 + C	α (mean)	0.0046±0.0009	0.0021±0.0004	0.0933±0.0970	0.0179±0.0169
	ln α (fit)	−3.37 - 3034/T	−4.501–2503/T	−16.118 + 19677/T	−7.419 + 4768/T
	α (at 1500 K)	0.0045	0.0021	0.0498	0.0144
SiC (Nor.) + Al_2O_3 + Si	α (mean)	0.1635±0.1544	0.2226±0.2799	0.0470±0.0344	0.3683±0.1951
	ln α (fit)	−18.932 + 24468/T	−24.23 + 33270/T	−15.423 + 17532/T	−5.051 + 6142/T
	α (at 1500 K)	0.0728	0.1287	0.0239	0.3843

[a] Mean value calculated whatever is the temperature of measurements.

norton $SiC + Al_2O_3$ bed, the gas phase is supersaturated only with Al_2O meanwhile for the carborundum $SiC + Al_2O_3$ bed, the gas-phase is super saturated with Al, Al_2O and CO. Combining these coefficients in order to compare the two beds, we conclude that the partial pressures over the Norton bed are lower than over the Carborundum bed as measured by direct comparison in the preceding paper.[2] The reason for these differences cannot come from the impurity contents since the Si(or SiO_2) or C small excess and impurities are vaporized at the beginning of the experiments as studied in the preceding paper,[2] the loss of these excess being part of the vaporization processes that led quickly to the congruent vaporization state. In addition, as the Norton and SiC powders have quite similar morphologies[2] (grain size and distribution) differences in evaporation and condensation coefficients cannot be attributed to differences in the real vaporization surface, but more probably to intrinsic surface defects nature and density. Indeed, kinks or dislocation edges are known to favor the transfer of molecules or atoms from the bulk to the gas phase. The surface characteristics have to be related to the production process of these powders.

Table 7
Ratios of evaporation α_i to condensation β_i coefficients as determined for each gaseous species and for different powder beds at 1500 K

α_i/β_i	Al	Al_2O	SiO	CO
SiC (Nor.) + Al_2O_3	1.02	2.47	0.55	0.4
SiC (Car.) + Al_2O_3	1.31	3.42	0.11	3.59
SiC (Nor.) + Al_2O_3 + C	0.35	0.53	2.26	0.68
SiC (Nor.) + Al_2O_3 + Si	2.59	5.88	1.73	3.4

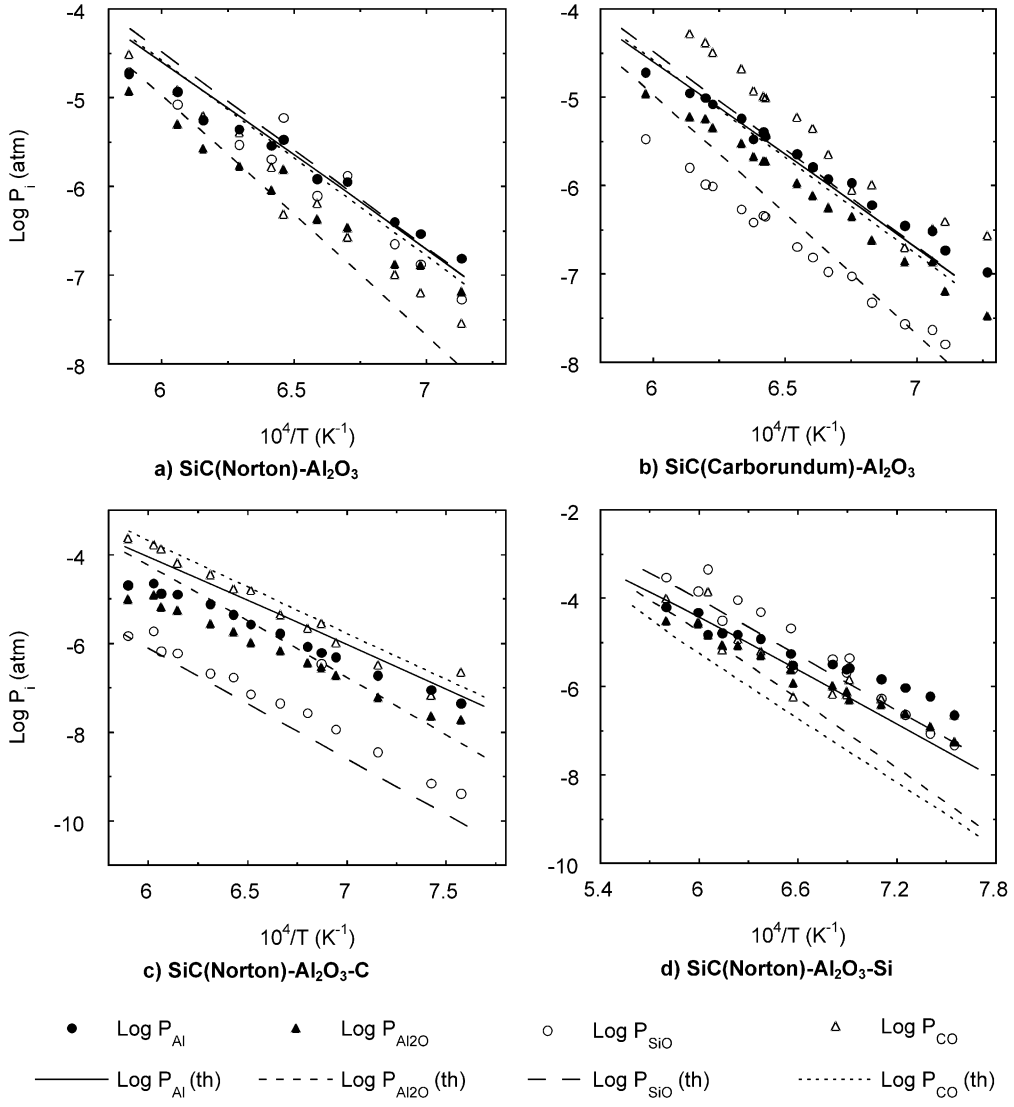

Fig. 3. Comparison of the decimal logarithm of our measured partial pressures p_m(i), as corrected by the condensation coefficients previously determined (Table 5), with the theoretical partial pressures as determined by thermodynamic calculations for congruent equilibrium conditions. •p(Al), ▲ (Al_2O), o p(SiO), Δ p(CO): experimental data (single cell experiment) corrected using β from Table 5. —— Al(g), - - - - Al_2O(g), – – SiO(g), ...CO(g): thermodynamic calculations.

The behavior of the two triphasic powder beds is very different: the silicon enhances all the partial pressures, meanwhile the carbon favors only SiO(g). In addition, the behavior of the SiC–Al_2O_3 beds remain very different from the triphasic powder beds.

4. Conclusions

The quantitative vaporization study of the SiC–Al_2O_3 powder beds, as well as those enriched with C or Si showed that any of these powders vaporizes at equilibrium. The vaporization and the condensation processes of their vapors, Al(g), Al_2O(g), SiO(g) and CO(g) are kinetically hindered, and the evaporation and condensation coefficients have been determined using Mass Spectrometry with the multiple Knudsen cell method. We have to quote that these coefficients are gross coefficients, that take into account the powder morphology as already discussed[24] for Si_3N_4. Consequently their values cannot be referred to specific crystal surfaces.

The existence of evaporation and condensation coefficient values that are systematically different leads to gas phases that may be supersaturated or undersaturated depending on the gaseous species considered as soon as the sintering process occurs in a quite closed container similar to Knudsen cells and with a neutral gas (Ar). According to our study, the gas phase over the SiC carborundum–Al_2O_3 beds is supersaturated with Al(g), Al_2O(g) and CO(g) in contrast to the SiC norton–Al_2O_3 beds where the gas phase is only supersaturated with Al_2O(g), and this feature must be related to better densification with a carborundum SiC bed.[25] In order to check if a general supersaturation initiates a better densification in the sintering process, we tried to add silicon to the beds in a sintering experiment, but we were not successful and the mass losses were important.[25] Thus, increasing all the partial pressures by appropriate beds does not improve the density in the sintering process. As a conclusion of the mass spectrometric observation of the vaporization and condensation behaviour of each gaseous species, the criteria for the choice of a powder bed as well as its environmental conditions are to obtain higher partial pressures of Al(g) and Al_2O(g) in combination with a high p_{CO}/p_{SiO} ratio. This conclusion agrees with the Mulla and Krstic[26] works in which a CO(g) pressure imposed of 0.1 MPa led to good densification.

References

1. Baud, S., Thevenot, F., Pisch, A. and Chatillon, C., High temperature sintering of SiC with oxide additives: I—thermodynamic analysis of the vaporization in the SiC–Al_2O_3 and SiC–Al_2O_3–Y_2O_3 systems. *J. Eur. Ceram. Soc.* (in press).
2. Baud, S., Thevenot, F., and Chatillon, C., High temperature sintering of SiC with oxide additives. II- Vaporization processes of powder beds and gas phase analysis by mass spectrometry. *J. Eur. Ceram. Soc.* (in press).
3. Rocabois, P., Chatillon, C. and Bernard, C., Vapour pressure and evaporation coefficient of SiO (amorphous) and SiO_2(s)+-Si(s) mixtures by the multiple Knudsen cell mass spectrometric method. *Rev. Int. Hautes Tempér. Réfract. Fr*,1992–1993, **28**, 37–48.
4. Inghram, M. G. and Drowart, J., Mass spectrometry applied to high temperature chemistry. In *High Temperature Technology*. MacGraw Hill, New York, 1959, pp. 219–240.
5. Drowart, J., Mass spectrometric studies of the vaporization of inorganic substances at high temperatures. In *Condensation and Evaporation of Solids* ed. E. Rutner P. Goldfinger and J. P. Hirth. Gordon and Breach, London, 1962, pp. 255–310.
6. Hilpert, K., High temperature mass spectrometry in materials research. *Rapid Comm. Mass Spectrometry*, 1991, **5**, 175–187.
7. Stolyarova, V. L., High temperature mass spectrometry study of oxide systems and materials. *Rapid Comm. Mass Spectrometry*, 1993, **7**, 1022–1032.
8. Hultgren, R. *et-al*, Selected Values of the Thermodynamic Properties of the Elements. *Amer. Soc. For Metals, Metals Park OH* 44073, 1973.
9. Freund, R. S., Wetzel, R. C., Shul, R. J. and Hayes, T. R., Cross-section measurements for electron-impact ionization of atoms. *Phys. Rev. A*, 1990, **41**, 3575–3595.
10. Chatillon, C., Private Communication issued from study of Ga_2O_3 vaporization.
11. Freund, R. S., Wetzel, R. C. and Shul, R. J., Measurements of electron-impact-ionization cross sections of N_2, CO, CO_2, CS, S_2, CS_2, and metastable N_2. *Phys. Rev. A*, 1990, **41**, 5861–5868.
12. Chase, M. W., Davies, C. A. and Downey, J. R., et al., JANAF thermochemical tables, 3rd edn. *J. Phys. and Chem. Ref. Data*, 1985, **14** (Suppl. 1).
13. Gurvich, L. V., Veyts, I. V. and Alcock, C. B., eds., *Thermodynamic Properties of Individual Substances, 4th edn*. English edn., Vols. 1 and 2. (Hemisphere Pub. Corp.), London, 1990.
14. Barin, I., *Thermochemical Data of Pure Substances*. VCH Weinken D-6940, Germany, 1993.
15. Ansara, I., Aims and achievements of the Scientific Group Thermodata Europe. In *Thermodynamic Modeling and Materials Data Engineering*, ed. Caliste J.P., Truyol A., Westbrook J.H. Springer-Verlag, Berlin, 1998, pp. 33–38.
16. Hirth, J. P. and Pound, G. M., Coefficients of evaporation and condensation. *J. Phys. Chem.*, 1960, **64**, 619–626.
17. Rosenblatt, G. M., Surfaces. In Treatise on Solid-state Chemistry VI, ed. N. B. Hannay. Plenum Press, New York, pp. 165–239 (Chapter 3).
18. Motzfeld, K., The thermal decomposition of sodium carbonate by the effusion method. *J. Phys. Chem.*, 1955, **59**, 139–147.
19. Whitman, C. I., On the measurements of vapor pressures by effusion. *J. Chem. Phys.*, 1952, **20**, 161–164.
20. Chatillon, C., Rocabois, P. and Bernard, C., High temperature analysis of the thermal degradation of silicon-based materials: I—binary Si-O, Si-C, Si-N compounds. *High Temp. High Press.*, 1999, **31**, 413–432.
21. Rosenblatt, G., Interpretation of Knudsen vapor-pressure measurements on porous solids. *J. Electrochem Soc.*, 1963, **110**, 563–569.
22. Chatillon, C., 2000. Evaporation and condensation coefficients by the multiple Knudsen cell mass spectrometric method. In *Proc. of Xth Int. IUPAC Conf. on High Temp. Mat. Chem.,* 10–14 April 2000. Forschungszentrums Jülich, Germany, pp. 403–406.
23. Dreger, L. H., Dadape, V. V. and Margrave, J. L., Sublimation and decomposition studies on boron nitride and aluminium nitride. *J. Phys. Chem.*, 1962, **66**, 1556–1559.

24. Rocabois, P., Chatillon, C. and Bernard, C., Thermodynamics of the Si–O–N system. I—high temperature study of the vaporization behaviour of silicon nitride by mass spectrometry. *J. Amer. Ceram. Soc.*, 1996, **79**, 1351–1360.
25. Baud S., Frittage en phase liquide du carbure de silicium: évolution des microstructures et des propriétés mécaniques. Etude thermodynamique des interactions oxydes SiC. PhD at Ecole Nationale Supérieure des Mines de Saint-Etienne and at Institut National Polytechnique de Grenoble, France, 9 March 2000.
26. Mulla, M. A. and Krstic, V. D., Pressureless sintering of β-SiC with Al_2O_3 additions. *J. Mater. Sci.*, 1994, **29**, 934–938.